OPEN

Precision Medicine Starts With Preanalytics: Real-Time Assessment of Tissue Fixation Quality by Ultrasound Time-of-Flight Analysis

Melissa L. Lerch, PhD, Daniel R. Bauer, PhD,† David Chafin, PhD,† Abbey Theiss, MS,† Michael Otter, MS,† and Geoffrey S. Baird, MD, PhD**

Abstract: Personalized medicine promises diagnosis and treatment of disease at the individual level and relies heavily on clinical specimen integrity and diagnostic assay quality. Preanalytics, the collection and handling steps of a clinical specimen before immunohistochemistry or other clinical assay, are critically important to enable the correct diagnosis of disease. However, the effects of preanalytics are often overlooked due to a lack of standardization and limited assessment tools to quantify their variation. Here, we report a novel real-time ultrasound time-of-flight instrument that is capable of monitoring and imaging the critical step in formalin fixation, diffusion of the fixative into tissue, which provides a quantifiable quality metric for tissue fixation in the clinical laboratory ensuring consistent downstream molecular assay results. We analyzed hundreds of tissue specimens from 34 distinct human tissue types and 12 clinically relevant diseased tissues for diffusion and fixation metrics. Our measurements can be converted into tissue diffusivity constants that correlate with the apparent diffusion constant calculated using magnetic resonance imaging ($R^2 = 0.83$), despite the differences in the approaches, indicating that our approach is biophysically plausible. Using data collected from time-of-flight analysis of many tissues, we have therefore developed a novel rapid fixation program that could ensure high-quality downstream assay results for a broad range of human tissue types.

Key Words: formalin fixation, ultrasound, time-of-flight, biospecimen, preanalytics

(*Appl Immunohistochem Mol Morphol* 2017;25:160–167)

For correct diagnosis of disease in surgical tissues, tissue fixation using aqueous formaldehyde (formalin) is a key preanalytic step in clinical testing, but despite formalin fixation's long history we lack a complete understanding of the fixation process. We have found optimizing formalin fixation can lead to improvements over standard practice, in particular in identifying tissue phosphoproteins that are important in the development of companion diagnostics in the drug development pipeline.[1] Prior efforts aimed towards studying or improving the quality of formalin fixation have focused either on altering a fixation protocol recipe (ie, changing the composition or temperature of formalin, or altering the time of incubation),[2–11] studying fixation statically by assessing tissue morphology or other features after fixation,[2,12] or measuring the quality of fixation post hoc by assessing putative indicator markers[9] such as RNA integrity that may act as a proverbial "canary in a coal mine." Each of these approaches, however, has shortcomings. Altered fixation protocols do improve the fixation quality of tissue with regards to some downstream analyses, but one-size-fits-all fixation protocols generally require fixation conditions lengthy or strong enough to fix even the most difficult tissue specimens, meaning that easier to fix tissues spend more time than necessary in fixative, lengthening assay turnaround time and possibly overexposing analytes to fixative. Static, post hoc studies of fixation quality likewise do not produce actionable information during a tissue fixation protocol, at a time where intervention (ceasing or prolonging fixation, if needed) is possible. Finally, the utility of tissue fixation quality indicators is limited by the fact that no completely generalizable molecular indicator of tissue quality is known, because the quality or preservation of any one of the thousands of potential tissue analytes cannot be assumed to predict accurately the preservation

Received for publication November 10, 2016; accepted November 15, 2016.

From the *Department of Laboratory Medicine, University of Washington, Seattle, WA; and †Ventana Medical Systems Inc., Tucson, AZ.

M.L.L. and D.R.B. contributed equally.

Supported by Ventana Medical Systems Inc. D.R.B., D.C., A.T., M.O. are employees of Ventana Medical Systems Inc. M.L.L. and G.S.B. receive research funding from Ventana Medical Systems Inc.

The authors declare no conflict of interest.

Reprints: Geoffrey S. Baird, MD, PhD, Laboratory Medicine, University of Washington, P.O. Box 359743, 325 9th Avenue, Seattle, WA 98104 (e-mail: gbaird@u.washington.edu).

Supplemental Digital Content is available for this article. Direct URL citations appear in the printed text and are provided in the HTML and PDF versions of this article on the journal's Website, www.appliedimmunohist.com.

of all of the other known or unknown potential tissue analytes. Thus, we believe that real-time biophysical monitoring of tissue fixation addresses an unmet need in both clinical medicine as well as tissue-based research for ensuring consistent results in molecular assays.

In prior work, we have shown that a formalin fixation protocol comprised of a preincubation in cold (4 ± 3°C) formalin followed by a short incubation in hot (45°C) formalin reduces the overall time needed for adequate fixation for a host of tissue types and allows preservation of highly labile tissue biomarkers such as phosphorylated proteins.[1,12] Because the evidence we collected in these prior studies indicated that the predominant process occurring during the cold formalin preincubation was formaldehyde diffusion into the tissue without significant cross-linking activity, in contrast to the rapid cross-linking observed during the warm step, we chose to focus our fixation monitoring efforts on observing the diffusion of formaldehyde into a broad array of human tissues at 6°C. We therefore report here the application of a time-of-flight (TOF) tissue fixation monitoring device[13] to a large number of tissue types relevant to the practice of general surgical pathology and crucial for correct diagnosis of disease in molecular assays. The time courses of formalin diffusion at 6°C help explain our prior demonstration of improved phosphoprotein preservation with rapid cold/hot fixation, and also indicate that real-time monitoring of formalin diffusion in tissue samples could be the basis of a novel biospecimen quality metric to ensure high-quality results in a variety of molecular assays.

TABLE 1. Time-of-Flight Data for Normal Human Tissue

	Decay Constant (h)		Decay Amplitude (nanosecond)	
Tissue	**Average**	**SD**	**Average**	**SD**
Adrenal gland	1.75	NA	28.1	NA
Appendix	1.69	0.36	23.1	1.0
Artery	0.54	0.21	8.7	4.1
Bladder	1.68	0.32	36.3	14.0
Brain	2.56	0.53	45.2	7.6
Breast	1.38	1.21	39.9	11.6
Cardiac	2.09	0.38	41.8	7.4
Cervix	1.36	0.15	44.8	14.1
Colon	1.37	0.58	36.0	9.4
Duodenum	2.02	0.44	48.4	21.5
Esophagus	1.85	0.07	65.2	1.4
Fat	3.69	2.47	25.0	13.2
Gallbladder	0.80	0.12	25.9	2.5
Ileum	1.46	0.00	32.5	1.5
Jejunum	1.33	0.05	35.7	0.7
Kidney	1.13	0.23	30.2	7.9
Liver	3.23	0.86	19.1	3.0
Lung	1.06	0.21	17.2	5.6
Lymph node	1.96	0.31	24.1	5.8
Muscle	1.01	0.23	23.7	8.1
Ovary	1.08	0.13	27.1	12.9
Pancreas	1.13	0.16	33.1	7.1
Prostate	1.27	0.19	19.1	4.7
Rectum	1.19	0.04	24.1	3.6
Ribcage	1.14	0.50	16.5	0.6
Skin	2.60	1.65	39.0	12.6
Spleen	3.36	0.56	28.5	8.2
Stomach	1.16	0.29	21.1	9.2
Testis	1.40	0.25	38.3	0.8
Thyroid	1.40	0.23	33.3	8.6
Tongue	1.90	NA	37.0	NA
Tonsil	2.75	0.54	30.3	5.5
Uterus	1.56	0.04	41.9	3.2

GI indicates gastrointestinal; NA, not applicable.

MATERIALS AND METHODS

Tissue Collection and Processing

Tissue leftover from clinical cases was collected under an exemption of consent by University of Washington's Institutional Review Board, and supplied as deidentified material by University of Washington Northwest Biotrust. Samples (Table 1) were collected fresh from surgical excisions, and periodically from autopsy material when surgical material would be difficult to obtain for research to be done on discarded material (ie, brain tissue from rapid autopsy). TOF measurements were done using mesh biopsy cassettes (CellSafe5 Biopsy cassette; CellPath USA) to measure multiple samples at once. All tissues were collected as 6-mm punches (Militex Biopsy punch), or as 6-mm cubes using scalpels (Militex #10).

Tissue fixed for 24 hours were submitted to University of Washington pathology department for standard tissue processing. Tissue fixed for rapid 6 + 1 protocol (explained below) were processed on Lynx II Tissue Processor (Electron Microscopy Sciences, Hatfield, PA) using standard reagents (Richard-Allan Scientific neutral-buffered formalin; Decon ethanol; Fisher Bioreagent Ethylene glycol; Fisher Methanol, EMS Low-melt paraffin embedding wax). The tissue was incubated for 6 hours in 4°C formalin, followed by 1 hour in 45°C formalin. Then samples were incubated in 70% ethanol for a variable-length fixation followed by 2 × 90% ethanol (20°C, 1 h), 3 × 100% ethanol (20°C, 1 h), 2 × xylene (20°C, 1 h), xylene (45°C, 90 min), wax (65°C, 1 h).

Automated Immunohistochemistry

Immunohistochemistry assays were performed on VENTANA Discovery XT automated staining instrument according to manufacturer's instructions. Slides were deparaffinized using EZprep solution (Ventana Medical Systems Inc., Tucson, AZ) 30 minutes at 75°C. Epitope retrieval was accomplished on the automated stainer with CC1 solution (Ventana Medical Systems Inc.) for 64 minutes at 95°C. Samples were stained with prediluted antibodies to cytokeratin 20 (clone SP33; #790-4431) and villin (clone CWWB1; #760-4277) on a VENTANA Discovery XT automated staining instrument according to manufacturer's instructions (Ventana Medical Systems Inc.). Optiview 3,3' diaminobenzidine detection kit (Ventana Medical Systems Inc.) was used. Briefly, steps included inhibitor for 8 minutes, linker for 8 minutes, multimer for 12 minutes, 3,3' diaminobenzidine/peroxide for 8 minutes, and copper for 4 minutes. Slides were then counterstained with hematoxylin II for 8 minutes (Ventana Medical Systems Inc.).

TOF Measurement and Calculation

To detect the small acoustic phase retardation resulting from formaldehyde diffusion into tissue, we developed a digital acoustic interferometry algorithm that calculated TOF differentials with subnanosecond precision.[13] Pairs of 4 MHz focused transducers were spatially aligned and tissue samples were placed near their common foci. The transmitting transducer was programmed to send out a sinusoidal pulse that was detected by the receiving transducer after traversing the formalin and tissue and the received pulse was used to calculate the transit time. A baseline TOF was acquired by measuring the signal through formalin and subtracting that value from the TOF with the tissue present to isolate the phase retardation from the tissue and to compensate for environmentally induced fluctuations in the formalin.

As formalin diffused into the tissue and replaced exchangeable fluid within the sample the overall composition of the tissue was slightly altered. As faster formalin diffused into the sample the tissue's net sound velocity increased resulting in a small decrease to the TOF. In practice, the TOF change from cold formalin diffusion was well correlated with a single-exponential decay. Mechanical scanning of the transducer pairs enabled 2-dimensional diffusion imaging.

Diffusivity Constant Calculation

Diffusivity constants were calculated from the TOF signals by modeling the rate at which formalin penetrates tissue according to the heat equation. The effect passive diffusion would have on the detected TOF signal was then modeled and a diffusivity constant that produced a TOF curve similar to the experimental one was determined to be the true diffusivity constant of the tissue. Initially, the thickness of the tissue was recorded and the speed of sound of the formalin was calculated from the reference channel acquisition. The sound velocity of the undiffused tissue [$r_{\text{tissue}}(t = 0)$] was then calculated according to:

$$\frac{1}{r_{\text{tissue}}(t=0)} = \frac{1}{r_{\text{nbf}}} + \frac{\Delta t}{d_{\text{tissue}}},$$

where, $\triangle t$ is the differential between the TOF through the formalin and tissue and TOF through only the formalin. Next, the spatial dependence of the reagent's concentration was simulated within the tissue through the solution to the heat equation solved for a cylindrical tissue:

$$c_{\text{nbf}}(t, D, x) = c_{\max}\left(1 - 2\sum_{n=1}^{\infty} \frac{e^{-D\alpha_n^2 t/R_0^2} J_0(\alpha_n x/R_0)}{\alpha_n J_1(\alpha_n)}\right),$$

where, x is the spatial coordinate in the depth direction of the tissue, R_0 is the radius of the sample, D is the candidate diffusivity constant, t is time, J_0 is a Bessel function of the first kind and 0th order, J_1 is a Bessel function of the first kind and 1st order, α_n is the location of the nth root of a 0th order Bessel function, and $c_{\max}$ is the maximum concentration of the reagent. According to the above equation, the concentration of the formalin was calculated at every time point of the experiment, for a range of biologically relevant diffusivity constants ($0.01 < D < 2\,\mu m^2/ms$), and at all positions within the tissue.

The TOF is an integrated signal across the entire tissue, the simulated concentration of formalin was integrated to calculate the total amount of formalin detected by ultrasound (c_{detected}). Using the total detected formalin, the expected TOF signal from each diffusivity constant was converted into candidate TOF signals according to:

$$TOF_{\text{cand}}(t, D_1) = \frac{d_{\text{tissue}}}{r_{\text{tissue}}(t=0) + \rho c_{\text{detected}}(t)\left(r_{\text{tissue}}(t=0) - r_{\text{reagent}}\right)},$$

where, D is tissue diameter, ρ is tissue porosity, r_{nbf} is sound velocity of formalin, r_0 is sound velocity of undiffused tissue,

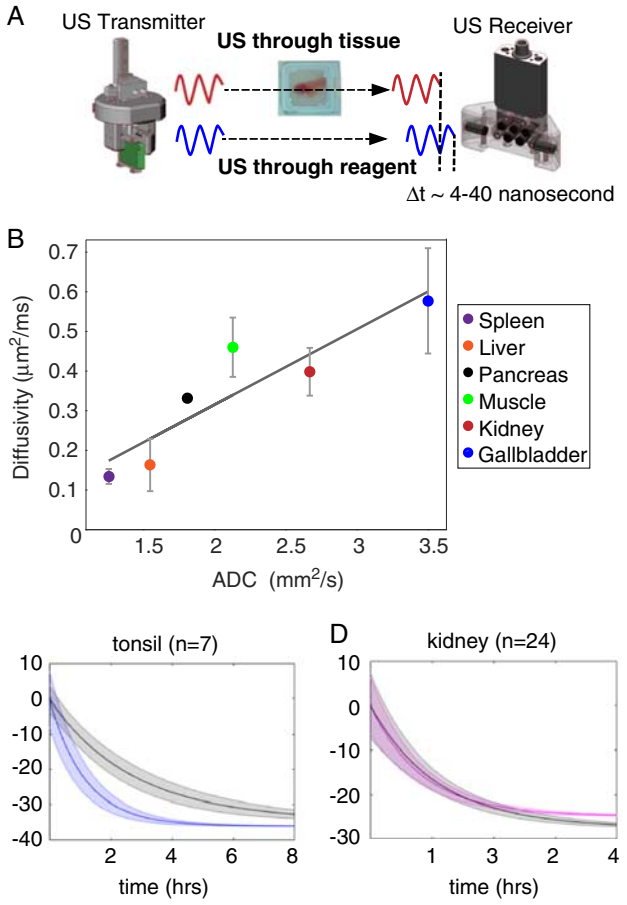

FIGURE 1. Acoustic time-of-flight (TOF) diffusion monitoring system. A, Solidworks drawing of scan head with pairs of 4-MHz transducers spatially aligned on either side of the green histologic cassette, which was vertically translated to acquire 2-dimensional information. Transit times of the acoustic pulses traversing the formalin and tissue (top) and a reference acquisition through formalin (bottom). B, Diffusivity coefficients for 6 tissues correlated to magnetic resonance imaging-derived apparent diffusion coefficients (ADC) with $R^2 = 0.83$. C, TOF trace for cold neutral buffered formalin diffusing into tonsils (gray) and non–cross-linking methanol (blue); ± SD is represented by shading. D, TOF trace for cold neutral buffered formalin diffusing into kidney (gray) and non–cross-linking ethylene glycol (red); ± SD is represented by shading.

and c is concentration of exogenous cross-linking agent which varied in time (t) and space (r).

The multitude of TOF_{cand} were then fit to a single exponential curve and the candidate decay constants compared with the decay constant of the experiment TOF signal in a least squares manner. The modeled diffusivity constant closest to the experimental TOF curve was called the true diffusivity constant.

RESULTS

A schematic of the TOF instrument, fully described elsewhere,[13] is shown in Figure 1A. A horizontal array of ultrasound transducers is scanned repetitively across tissue submersed in fixative, and the TOF of ultrasound waves is measured with nanosecond accuracy, representing the rate of fixative diffusion. Through computational modeling, TOF diffusion curves were used to generate fixative diffusivity coefficients that were well correlated with magnetic resonance imaging-derived apparent diffusion coefficients of water[14] ($r^2 = 0.83$, error bars represent SD) indicating that the 2 orthogonal methodologies yield data that trend consistently (Fig. 1B). Changes in TOF over time from incubations of tonsil (Fig. 1C) and kidney cortex (Fig. 1D) in 6°C formalin [10% neutral-buffered formaldehyde (CH_2O); gray lines], 10% methanol (CH_3OH) in phosphate-buffered saline (blue line in Fig. 1C) or 10% ethylene glycol [$(CH_2OH)_2$] in phosphate-buffered saline (red line in Fig. 1D) indicate that small molecules similar in size and functionality to the molecular species predominant in neutral-buffered formaldehyde [methylene glycol, $CH_2(OH)_2$] exhibit similar TOF trends. As these trends are similar even for small molecules that cannot cross-link proteins, the trends in TOF observed appear to be largely, if not entirely, due to diffusion of solvents and not due to cross-linking activity.

To build on our prior findings that a rapid cold-hot fixation protocol yielded excellent histomorphology,[12] we collected diffusion data with the new TOF-enabled fixation instrument. Colon punch biopsy specimens (6 mm) were placed into cold (6°C) formalin for 6 hours (point shown in TOF trace Fig. 2A) and then placed into hot (45°C) formalin for 1 hour, followed by standard tissue processing (dehydration and wax infiltration). The long cold incubation allows the formaldehyde to penetrate to the center of the tissue with a minimum of cross-linking, then a short hot incubation allows for quicker cross-linking to occur throughout the tissue leading to more homogenous fixation even in large portions of tissue. Tissue fixed for 24 hours in room temperature formalin was compared with the rapid fixation condition using Hematoxylin and eosin staining as well as immunohistochemistry for cytokeratin and villin (Fig. 2B). Results confirmed that the TOF-enabled instrument using a rapid fixation protocol yields similar results to the standard 24-hour fixation protocol prevalent in the clinical laboratory.

TOF data were then collected from 34 different clinically relevant tissues (Fig. 3 and Table 1) using 6-mm pieces of tissue. We selected the tissue size of 6 mm to represent the maximum dimension of tissue that reasonably fits into a tissue cassette, yet might take longer for formalin to penetrate. The majority of tissue was obtained from surgical procedures and ischemic time (cold and warm) was consistent with typical procedures found in the hospital pathology labs. However, some tissues were obtained from autopsies because it was not practical to obtain otherwise (ie, brain). In the case of autopsy tissues, the postdeath interval extended up to 72 hours. Representative TOF traces are shown from tissues with fast, intermediate, and slow apparent diffusion (gallbladder, lymph node, spleen, Figs. 3A–C). Tissues for which long fixation times have been recognized

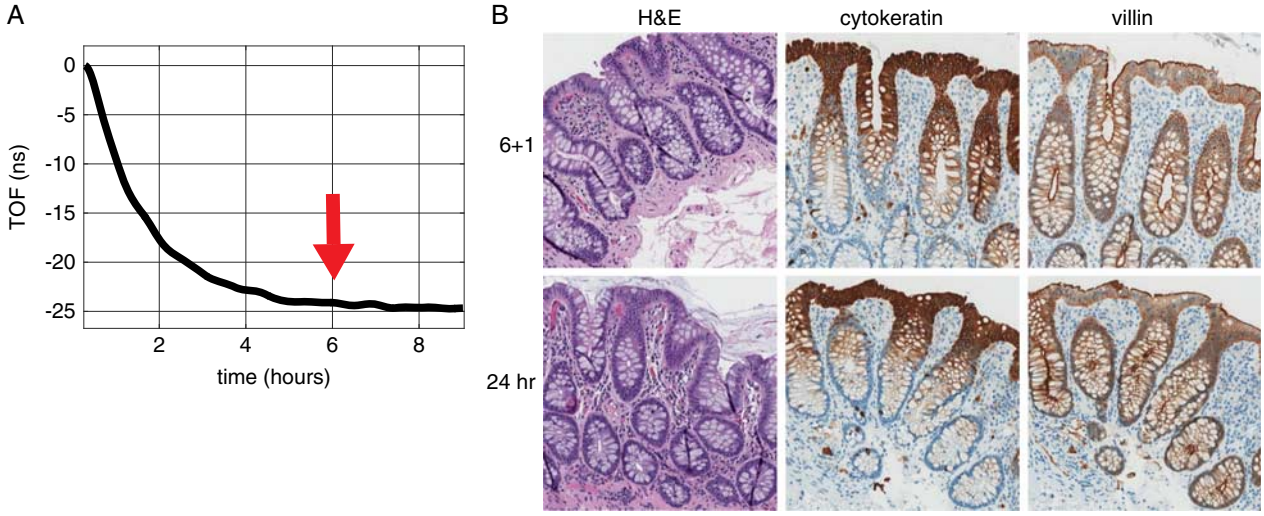

FIGURE 2. Histomorphology and time-of-flight (TOF) trace of colon tissue. A, TOF trace for colon (red arrow indicates the time tissue transferred from cold to hot formalin). B, Immunohistochemistry (IHC) of the colon for 6+1 fixation (top row) and 24 hours fixation (bottom row) with H&E (first column), cytokeratin IHC (second column), and villin IHC (third column).

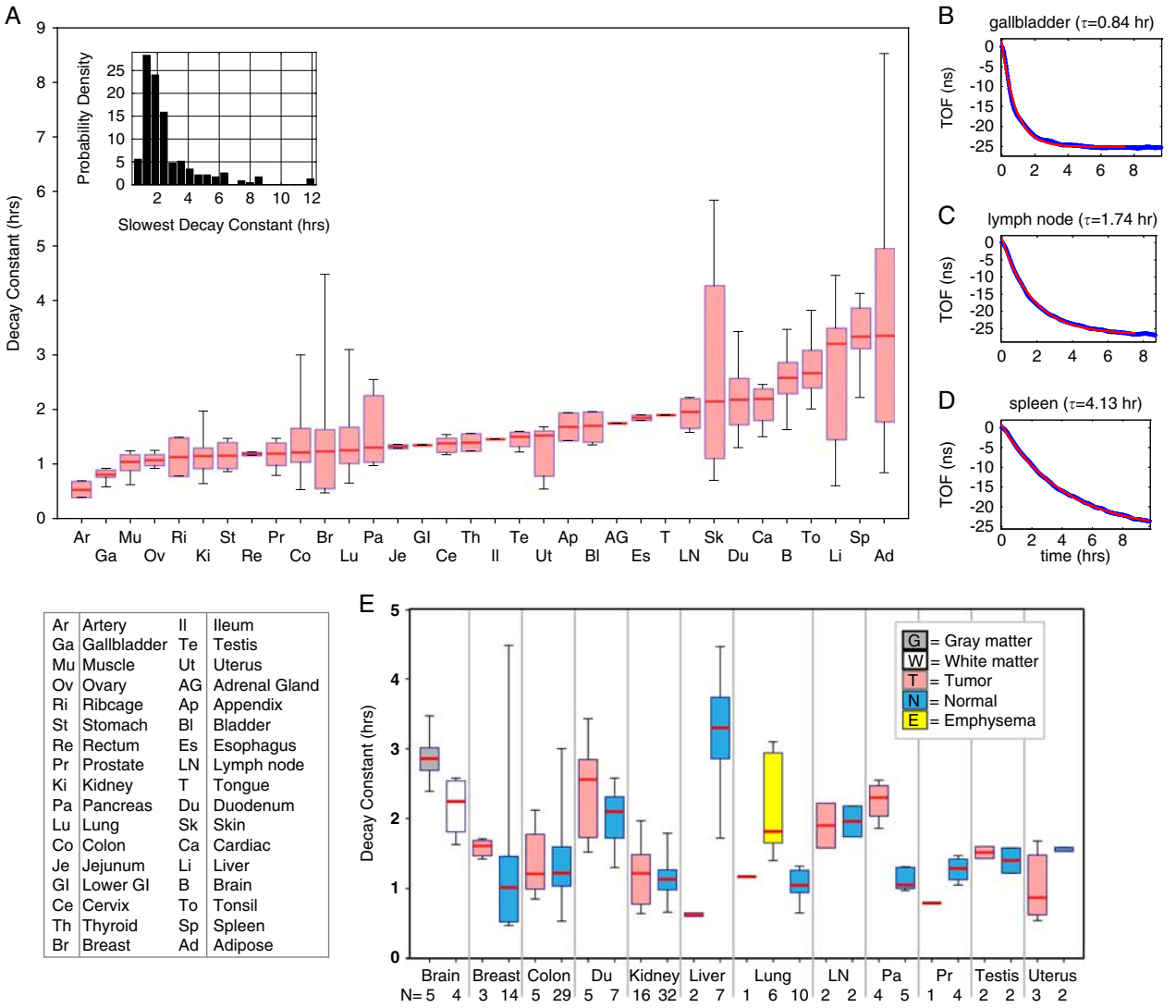

FIGURE 3. Time-of-flight (TOF) data for clinically relevant tissues. A, Median time of diffusion for 34 tissues demonstrating variability within and between tissue types; inset shows distribution of slowest pixel value of τ for all tissues. B, Fast diffusing gallbladder (τ = 0.84 h). C, Intermediate diffusion lymph node (τ = 1.74 h). D, Slow diffusing spleen (τ = 4.13 h). E, TOF data on 11 different tumor tissues matched with normal tissue, as well as normal brain tissue comparing white and gray matter.

to be necessary by histotechnologists from experience (fat and brain) are among those with the slowest observed fixative diffusion (longest decay constant), whereas mucosal surfaces and tissues with relative large surface area to volume ratios (gallbladder, rectum, and lung) were found to have faster diffusion. There is still a large variance in decay constants within tissue types, however, indicating that associating a single optimal fixation time to any given tissue type would not be prudent. Also, the slowest apparent fixative diffusion (decay constant) observed in any portion of a tissue specimen, shown in the inset of Figure 3D, demonstrates that there is heterogeneous formalin diffusion even within a single piece of tissue. This further indicates that active monitoring of formalin diffusion would be needed to ensure complete formalin diffusion to an entire specimen in the quickest time possible (Supplemental movie, Supplemental Digital Content 1, http://links.lww.com/AIMM/A148 shows the relationship between the TOF curve and diffusion across the entire tissue specimen). Finally, we collected apparent fixative diffusion data from 11 different tissue-specific carcinomas matched with normal tissue, white and gray brain matter, and lung tissue with emphysema (Fig. 3E and Table 2). The variability of apparent fixative diffusion observed across normal tissues and between normal tissues and associated tissue-specific neoplasms further emphasizes the variability in formalin diffusion across different tissue types and the need to treat each specimen individually when considering formalin fixation.

In practice, we envision a TOF-capable fixation instrument as part of a total quality system for histopathologic

TABLE 2. Time-of-Flight Values for Paired Disease and Normal Tissue

	Decay Constant (DC) (h)		Decay Amplitude (DA) (nanosecond)	
Tissue	**DC Average**	**DC SD**	**DA Average**	**DA SD**
Brain gray	2.87	0.39	47.1	7.3
Brain white	2.18	0.45	42.9	8.3
Breast tumor	1.58	0.15	28.5	6.1
Breast normal	1.38	1.21	39.9	11.6
Colon tumor	1.38	0.51	70.9	22.0
Colon normal	1.37	0.58	36.0	9.4
Duodenum tumor	2.39	0.76	62.4	21.0
Duodenum normal	2.02	0.44	48.4	21.5
Kidney tumor	1.18	0.42	25.9	10.2
Kidney normal	1.13	0.23	30.2	7.9
Liver tumor	0.63	0.04	27.6	7.5
Liver normal	3.23	0.86	19.1	3.0
Lung tumor	1.17	na	30.2	NA
Lung emphysema	2.12	0.72	27.0	7.0
Lung normal	1.06	0.21	17.2	5.6
Lymph node tumor	1.90	0.45	27.5	7.9
Lymph node normal	1.96	0.31	24.1	5.8
Pancreas tumor	2.25	0.30	34.2	9.3
Pancreas normal	1.13	0.16	33.1	7.1
Prostate tumor	0.79	NA	6.8	NA
Prostate normal	1.27	0.19	19.1	4.7
Testis tumor	1.52	0.12	55.6	2.8
Testis normal	1.40	0.25	38.3	0.8
Uterus tumor	1.03	0.59	21.3	7.4
Uterus normal	1.56	0.04	41.9	3.2

NA indicates not applicable.

analysis of biospecimens (Fig. 4A). Tissue can be collected into cold (4°C) formalin and incubated in the cold until fully permeated with formalin, as evidenced by images of TOF changes that are correlated to completion of formalin diffusion (Fig. 4B). Additional metrics derived from the TOF analysis shown in Figures 4C and D include the TOF decay amplitude (total change in ultrasound TOF, likely indicating diffusion of formalin into tissue) and the TOF decay constant (time constant, correlated with speed of diffusion across the tissue). After preincubation in 4°C formalin, subsequent rapid fixation in 45°C formalin[12] would be followed by tissue processing and dehydration steps, and thereafter sectioning, staining, and microscopic analysis.

DISCUSSION

It has been recognized for years that the preanalytical phase of testing is the stage at which most errors occur. As a key preanalytical process in tissue specimen preparation, formalin fixation is especially prone to errors that might affect downstream assays. Many tissue assays performed today involve at least 1 step that either attempts to undo formalin fixation, such as heat induced epitope retrieval,[15] or else steps that are known to rely critically on the length and intensity of formalin fixation, such as nucleic acid extraction. Dynamic TOF monitoring of formaldehyde diffusion into tissue specimens is thus the first technique to provide real-time monitoring and quality information of a preanalytical process that is ubiquitous and critical in clinical and research assays around the world. As those involved in laboratory quality improvement know, it is often said that, "you cannot improve it if you cannot measure it," and it is with this novel approach that we propose that tissue fixation can be measured.

A key and beneficial feature of the TOF monitoring is that the TOF images produced by the instrument are also a morphometric documentation of the tissue that was processed (ie, images in Fig. 4). Such documentation can be an invaluable tool for quality assurance in cases when the histologic process has resulted in a suspected specimen swap or a histologic "floater," as the tissue visualized on a histologic slide should match the appearance of the specimen that was fixed in the instrument.

The data presented here demonstrate that all human tissues so far studied have reproducible TOF curves with apparent first-order decays in keeping with predictions from Fick's law, indicating that TOF diffusion monitoring will be a reliable way to monitor the adequacy of fixative penetration into most, if not all, tissue types used in clinical or research assays. As we have demonstrated that TOF curves can be reproduced with non–cross-linking molecules such as methanol and ethylene glycol, we believe that the TOF curve derives mostly, if not entirely from solvent diffusion rather than cross-linking. Whether or not the TOF curve is due to the diffusion of formaldehyde/methylene glycol molecules or to the diffusion of the bulk solvent (water/phosphate-buffered saline) into tissue is not clear, but the evidence collected supports the idea that the TOF curve during cold incubation represents the movement of the fixative into

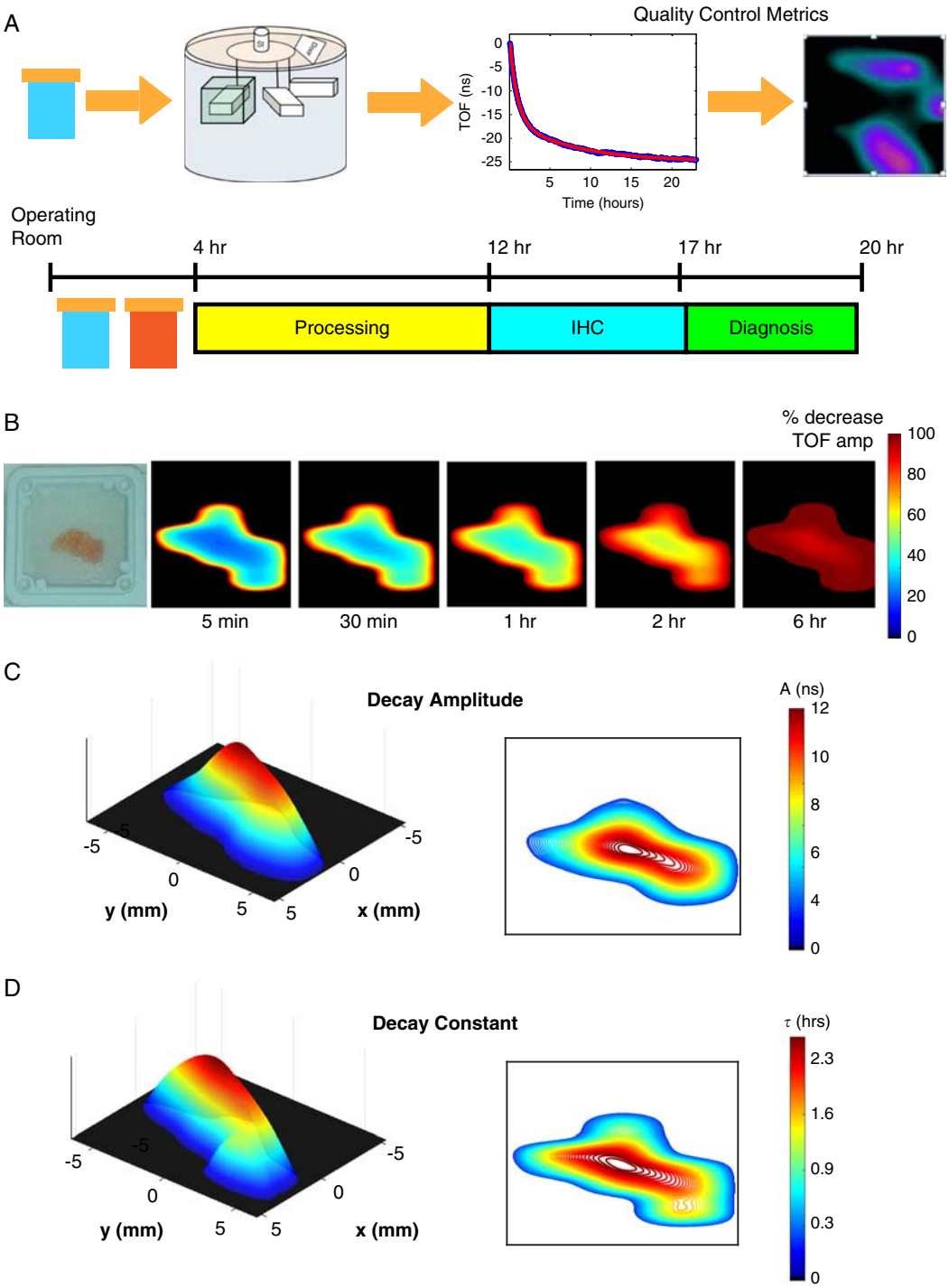

FIGURE 4. Quality control using time-of-flight (TOF) in the clinical pathology laboratory. A, Schematic of clinical workflow. B, Tonsil tissue in mesh cassette. 2D representation of 10% formalin diffusion into tissue over time visualized as percent decrease in TOF amplitude over time. C, 2D and 3D representation of the tonsil tissue decay amplitude (nanoseconds). D, 2D and 3D representation of the tonsil tissue showing τ, the decay constant (hours). 2D indicates two dimensional; 3D, three dimensional. IHC indicates immunohistochemistry.

tissue, whereas rapid cross-linking chemistry appears to be the dominant process occurring during hot formalin incubation as the equilibrium is shifted from methylene glycol to formaldehyde.

Although bone was not extensively studied here, we are actively investigating whether or not this same technique could be used to monitor the bone decalcification process and allow one to end the process as soon as possible, as many down-

stream molecular assays have been noted, anecdotally, to fail in bone specimens that have been subjected to lengthy decalcification.[16] Similarly, the TOF technique could likely be used to monitor downstream steps in tissue processing, such as dehydration and paraffin infiltration that are not currently believed to affect overall tissue quality, but may in fact be important. In addition, while the prototype fixation monitoring device described here only accommodates 1 sample at a time, future versions of this instrumentation could easily be designed to accommodate multiple tissue cassettes in either batched or random access configurations.

Initial studies have demonstrated a good correlation between the slope of the TOF curve at the time fixation is ceased and downstream histomorphologic quality (data not shown). Additional studies will be required to correlate TOF results with the quality of new and different assays, as it is not clear that the penetration of formalin required for any specific assay will be the same as that required for a different assay. One promising finding has been that TOF analysis has generally yielded results that indicate complete formalin diffusion over times that are essentially the same as those we have found to be correlated with excellent phosphoprotein preservation in colorectal carcinomas.[1] Regardless of specific assay sensitivities, however, it is clear that without a quantifiable parameter of tissue fixation such as that provided by the TOF instrument, no studies correlating the key preanalytical variable of formalin penetration with downstream assay results would even be possible.

Dynamic TOF monitoring provides additional benefits past the obvious provision of quantifiable metrics of fixative penetration. The fact that TOF measurements are made in real time means that future random-access tissue processing instrumentation could conceivably fix each tissue specimen precisely as much as is needed, ie, until the prescribed amount of formaldehyde penetration has occurred but no more, allowing analyses that are truly "personalized" to each portion of tissue from each patient.

ACKNOWLEDGMENTS

The authors thank Corinne Fligner, Heather Jennings, and Brian McGing for assistance with autopsy tissues. The authors thank the University of Washington Rapid Autopsy team members (funded by UW Alzheimer's Disease Research Center grant NIH P50 AG005136 for brain tissue), UW Genitourinary Cancer Specimen Biorepository, and patients and families that donated tissue.

REFERENCES

1. Theiss AP, Chafin D, Bauer DR, et al. Immunohistochemistry of colorectal cancer biomarker phosphorylation requires controlled tissue fixation. *Plos One*. 2014;9:6.
2. Looi LM, Loh KC. Microwave-stimulated formaldehyde fixation of experimental renal biopsy tissues: computerised morphometric analysis of distortion artefacts. *Malays J Pathol*. 2005;27:23–27.
3. Hafajee ZA, Leong AS. Ultra-rapid microwave-stimulated tissue processing with a modified protocol incorporating microwave fixation. *Pathology England*. 2004;36:325–329.
4. Ferris AM, Giberson RT, Sanders MA, et al. Advanced laboratory techniques for sample processing and immunolabeling using microwave radiation. *J Neurosci Methods*. 2009;182:157–164.
5. Boon ME, Marani E. The major importance of temperature data in publications concerning microwave techniques. *Eur J Morphol*. 1991; 29:184–185.
6. Boon ME, Gerrits PO, Moorlag HE, et al. Formaldehyde fixation and microwave irradiation. *Histochem J*. 1988;20:313–322.
7. Boon ME, Kok LP, Ouwerkerk-Noordam E. Microwave-stimulated diffusion for fast processing of tissue: reduced dehydrating, clearing, and impregnating times. *Histopathology*. 1986;10:303–309.
8. Leong AS, Duncis CG. A method of rapid fixation of large biopsy specimens using microwave irradiation. *Pathology*. 1986;18:222–225.
9. Cox ML, Schray CL, Luster CN, et al. Assessment of fixatives, fixation, and tissue processing on morphology and RNA integrity. *Exp Mol Pathol*. 2006;80:183–191.
10. Gillespie JW, Best CJ, Bichsel VE, et al. Evaluation of non-formalin tissue fixation for molecular profiling studies. *Am J Pathol*. 2002;160:449–457.
11. Nadji M, Nassiri M, Vincek V, et al. Immunohistochemistry of tissue prepared by a molecular-friendly fixation and processing system. *Appl Immunohistochem Mol Morphol*. 2005;13:277–282.
12. Chafin D, Theiss A, Roberts E, et al. Rapid two-temperature formalin fixation. *Plos One*. 2013;8:16.
13. Bauer DR, Stevens B, Chafin D, et al. Active monitoring of formaldehyde diffusion into histological tissues with digital acoustic interferometry. *J Med Imaging (Bellingham)*. 2016;3:1–9.
14. Chavhan GB, Alsabban Z, Babyn PS. Diffusion-weighted imaging in pediatric body MR imaging: principles, technique, and emerging applications. *Radiographics*. 2014;34:E73–E88.
15. Miller R, Swanson P, Wick M. Fixation and epitope retrieval in diagnostic immunohistochemistry: a concise review with practical considerations. *Appl Immunohistochem Mol Morphol*. 2000;8:228–235.
16. Choi SE, Hong SW, Yoon SO. Proposal of an appropriate decalcification method of bone marrow biopsy specimens in the era of expanding genetic molecular study. *J Pathol Transl Med*. 2015;49:236–242.